PERGAMON

International Journal of Solids and Structures 38 (2001) 5661–5677

INTERNATIONAL JOURNAL OF SOLIDS and STRUCTURES

www.elsevier.com/locate/ijsolstr

Stress based optimization of torsional shafts using an evolutionary procedure

Qing Li [a,1], Grant P. Steven [a,*], Osvaldo M. Querin [a], Y.M. Xie [b]

[a] *Department of Aeronautical Engineering, Engineering Faculty, Building J07, The University of Sydney, Sydney, NSW 2006, Australia*
[b] *School of Built Environment, Faculty of Engineering and Science, Victoria University of Technology, P.O. Box 14428, Melbourne City Mail Center, VIC 8001, Australia*

Received 23 February 2000

Abstract

This paper presents a shear stress based evolutionary algorithm for the cross-section design of shafts subject to torsion. In this method, finite element analysis is employed to find the shear stress distribution throughout the cross-sectional area of the shaft. To seek a full stress or iso-strength design, two basic procedures are developed in this paper; either progressively removing the least efficient material from the design domain or gradually shifting material from the least efficient (under-utilized) location to the most efficient (over-utilized) location while keeping the cross-sectional area constant. The former leads to the remaining material being more effectively utilized and the latter results in the material being more intelligently redistributed. The method proves to be simple in its physical concept and mathematical operations, and easy for computer implementation. A number of typical examples demonstrate that the proposed approach is effective in solving design problems for both simply-connected and multiply-connected cross-sections, involving reshaping of both interior and exterior boundaries.

Keywords: Finite element analysis; Torsional shaft; Evolutionary structural optimization; Shape optimization

1. Introduction

Structural optimization aims at achieving the best structural performance and material efficiency while satisfying certain constraints. In the past two decades, significant progress has been made in this area for a wide range of physical topics. The problem covered by this paper is the cross-sectional shape optimization of elastic shafts in torsion. As well as having significance from a purely mathematical point of view, such a problem is also of direct practical application in mechanical, civil, automotive and aeronautical engineering.

As a typical example of structural optimization, shape design of the torsional shaft has attracted extensive attention since the late 1940s. The earliest result appears to be Polya's proof (Polya, 1948) via a

* Corresponding author. Fax: +61-2-9351-4841.
E-mail addresses: qli@aero.usyd.edu.au (Q. Li), grant@aero.usyd.edu.au (G.P. Steven).
[1] Tel.: +61-2-9351-7129; fax: +61-2-9351-4841.

0020-7683/01/$ - see front matter
PII: S0020-7683(00)00365-6

regularization approach in 1948 that a circular bar has the highest torsional stiffness among all singly connected convex geometry of a given area. Furthermore, Polya and Weinsten (1950) showed that in the case of multiply connected cross-sections, a ring bounded by two concentric circles has the highest torsional stiffness. The same results were later proven by Banichuk (1976) using variational calculus. During the 70s and 80s, Karihaloo and his colleagues (Banichuk and Karihaloo, 1976; Parbery and Karihaloo, 1977, 1980 and Karihaloo and Hemp, 1983, 1987) conducted a series of analytical studies on the multi-purpose optimization of cross-sectional profiles for combined torsional and flexural rigidity. With the development of new composite materials, torsional shafts composed of multiple materials with non-homogeneous and anisotropic properties have also been widely investigated (Adali, 1981; Lurie et al., 1982; Mioduchowski et al., 1989 and Burns and Cherkaev, 1997).

One common point of the above mentioned research has been to solve the governing equation analytically. Although these solutions have significantly advanced the design theory of shafts and provided the benchmarks, there still exist difficulties in handling some more practical situations with complex geometric constraints and connectivity variations. For this reason, various numerical techniques have been developed by combining finite element (FE) methods (Dems, 1980; Hou and Chen, 1985 and Schramm and Pilkey, 1993) or more recently boundary element methods (Mota Soares et al., 1984; Gracia and Doblare, 1988 and Schramm and Pilkey, 1994) with mathematical programming techniques. In these numerical approaches, nodal coordinates or other boundary parameters are usually treated as the design variables. A cycle of FE or boundary element calculation, followed by sensitivity or other gradient calculations and mathematical programming is iteratively carried out until an optimal shape is found. Due to the suitability of finite elements and boundary elements to such complicated problems, this approach has shown significant advantages over the classical methods. To implement such procedures, however, gradient information, automatic remeshing and suitable non-linear programming algorithms are needed. These usually require considerable mathematical and computational effort. The latest progress made by Kim and Kim (2000) showed a successful extension of the homogenization method (Bendsøe, 1995) to the torsion problem, in which the remeshing process has been avoided.

This paper proposes a simple rule-based evolutionary structural optimization (ESO) procedure to resolve the traditional torsion shape and topology optimization problems. This approach employs finite element analysis (FEA) to determine the shear stress distribution for regions subject to torque. From the strength point of view, an excessive stress could reflect a potential structural failure while a low stress may mean an inefficient usage of material. Ideally, the stress levels throughout the entire design domains of the section are expected to be as close as possible to each other. This concept leads to a judgment, on the available design space of the cross-section, about which locations should have material present and which locations should have material removed. Like other numerical approaches, the optimum is only achieved in an iterative fashion consisting of two basic steps: FEA and modification of material distribution. Since the analysis region has been divided into many small elements, the material addition or subtraction can be simply represented by adding or removing elements in the FE model. In the computation, the property types of the elements are treated as design variables while shear stress levels of the element are considered as the optimality criterion. This does not require extra gradient information for mathematical programming, and it also avoids the use of intricate remeshing procedures. In this sense, the ESO method is simpler in its computer implementation and more flexible in its engineering applications.

2. Problem formulations and optimality criterion

In order to seek an optimum shape of the torsion section, it is essential to determine the structural response of torsion systems. From the Saint Venant theory of torsion, the elastic deformation of the sections can be described by Poisson's equation

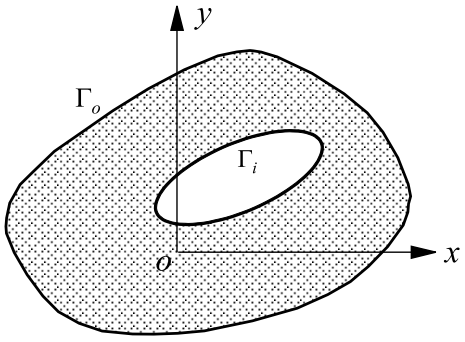

Fig. 1. Multiply connected design domain.

$$\frac{\partial}{\partial x}\left(\frac{1}{G_x}\frac{\partial \phi}{\partial x}\right)+\frac{\partial}{\partial y}\left(\frac{1}{G_y}\frac{\partial \phi}{\partial y}\right)+2\theta=0, \tag{1}$$

and the Dirichlet-type boundary conditions as illustrated in Fig. 1,

$$\begin{cases}\phi=0, & (x,y)\in \mathbf{\Gamma}_o,\\ \phi=C_i, & (x,y)\in \mathbf{\Gamma}_i,\end{cases} \tag{2}$$

where ϕ represents the Prandtl stress function, θ is the angle of twist per unit length, $\mathbf{\Gamma}_o$ and $\mathbf{\Gamma}_i$ $(i=1,2,\ldots,m)$ stand for the exterior and interior boundaries (m is the number of inner boundaries), and G_x, G_y respectively denote the shear moduli corresponding to x and y directions.

This is one form of the common elliptic equation in mathematical-physics. Although Eqs. (1) and (2) are of significant mathematical and physical interest and despite great efforts been devoted to solve them over the last two centuries, it is by no means easy to find theoretical or analytical solutions, in particular for complex geometry and multiple connectivity. To cope with such intricate problems as design optimization in which the shape or topology of analyzed region is continuously being modified, the FE or other numerical analysis methods are usually needed (Hinton and Owen, 1981; Huston and Passerello, 1984 and Rao, 1989).

In traditional solutions, the optimal problems are constructed either to minimize the weight or volume, or the cross-sectional area of a shaft subject to a prescribed torsional rigidity constraint (Banichuk and Karihaloo, 1976; Parbery and Karihaloo, 1977, 1980 and Karihaloo and Hemp, 1983, 1987) as

$$\begin{cases}\min & A=\min\int\int_A \mathrm{d}x\,\mathrm{d}y,\\ \text{s.t.} & \frac{2}{\theta}\int\int_A \phi\,\mathrm{d}x\,\mathrm{d}y-R^*\geqslant 0\end{cases} \tag{3}$$

or equivalently, to maximize the torsional rigidity subject to a prescribed weight, volume, or a given cross-sectional area constraint (Dems, 1980; Adali, 1981; Lurie et al., 1982; Mota Soares et al., 1984; Hou and Chen, 1985; Gracia and Doblare, 1988; Mioduchowski et al., 1989; Schramm and Pilkey, 1993 and Burns and Chekaev, 1997) as

$$\begin{cases}\max & R=\max\frac{2}{\theta}\int\int_A \phi\,\mathrm{d}x\,\mathrm{d}y,\\ \text{s.t.} & \int\int_A \mathrm{d}x\,\mathrm{d}y-A^*=0,\end{cases} \tag{4}$$

where $R=\frac{2}{\theta}\int\int_A \phi\,\mathrm{d}x\,\mathrm{d}y$ is the torsion rigidity, and A^* and R^* denote the imposed restrictions on cross-sectional area (in unit of m^2) and torsional rigidity (in unit of N/arc) respectively.

Obviously, such optimizations mainly reflect the rigidity aspects of a design, where the material is redistributed to ensure the stiffest design. In other circumstances, the designer may wish to impose a strength

criterion, e.g., to find an evenly or fully stressed design. For this purpose, an appropriate reference criterion related to material stress level is needed. FEA, directly provides the solution for nodal stress function ϕ and subsequently the elemental shear stress components $\tau_{xz} = \partial\phi/\partial y$ and $\tau_{yz} = -\partial\phi/\partial x$. One of the most frequently used measures of the material shear strength can be the resultant of shear stress components as (Hinton and Owen, 1981)

$$\tau = \sqrt{\tau_{xz}^2 + \tau_{yz}^2} = \sqrt{\left(\frac{\partial\phi}{\partial y}\right)^2 + \left(-\frac{\partial\phi}{\partial x}\right)^2}. \tag{5}$$

As a result, the resultant shear stress level is adopted to estimate the efficiency of material usage from the iso-strength standpoint in this study. A greater (or a smaller) elemental resultant stress level implies a higher (or a lower) efficiency of material usage.

3. Evolutionary structural optimization procedure

3.1. Procedure for the volume reduction

Typically, after FEA, the shear stress levels in some elements are quite lower than others. From the viewpoint of iso-strength or even stress, it is logical that such less efficiently utilized material should be gradually *removed* from the structure. In the ESO method, the criterion of element removal is determined by comparing elemental resultant shear stress τ^e with the highest τ^{max} or the mean $\bar{\tau}$ value over the entire analysis domain, i.e. an element is removed if it satisfies

$$\tau^e \leqslant \mathrm{RR_{SS}} \times \tau^{max}, \quad \text{or} \quad \tau^e \leqslant \mathrm{RR_{SS}} \times \bar{\tau}, \tag{6}$$

where $\mathrm{RR_{SS}}$ is called *Rejection Ratio*. The process of the element removal is repeated using the same value of $\mathrm{RR_{SS}}$ until there are no more elements that can be removed. This means that an ESO Steady State (SS) has been reached, by which the lowest stress level within the design domain has become greater than a certain percentage of the maximum or mean level. In order for the optimization process to continue at this stage, an Evolutionary Rate (ER) is introduced so that

$$\mathrm{RR_{SS+1}} = \mathrm{RR_{SS}} + \mathrm{ER}. \tag{7}$$

With the increased rejection ratio, the cycle of FEA and element removal takes place again until a new steady state is reached. A typical value for ER is around 1% to ensure a smooth change between two steady states.

As formulated in Eq. (2), in order to solve the boundary value problems of the elliptical Eq. (1), the conditions of the outer and the inner boundaries need to be considered separately. When the elements are removed from the outer boundary Γ_o, the stress function ϕ_i at the nodes of newly shaped boundary should always be updated to zero. This can be simply implemented by imposing the stress functions at all nodes of any removed element to zero; When the elements are removed from any old inner boundary or from the remaining interior regions of solid, the nodal stress functions ϕ_i $(i = 1, 2, \ldots, m)$ at the inner boundaries need to be set to some specific constants C_i $(i = 1, 2, \ldots, m)$. Obviously, this raises a difficulty in determining such boundary constants (Hinton and Owen, 1981). For this reason, element removal cannot directly follow traditional ESO procedure (Xie and Steven, 1993, 1997 and Li et al., 1999b). Furthermore, it is worth noticing that the former does not change the connectivity of the design domain, whereas the latter could. Generally speaking, the design of a multiply connected solid provides more extensive practical significance in enhancing structural performance and reducing material volume.

In multiply connected designs, to overcome the difficulty of determining the boundary stress functions, a *soft kill* technique proposed by Hinton and his colleagues (Hinton and Sienz, 1995) is adopted herein, whereby any internal hole is assumed to compose of a material with relatively low shear moduli G_x, G_y (say 1/1000 of the moduli of the solid material). In computation, the degraded modulus elements have thus negligible significance to the torsion capacity, and are therefore regarded as void in the structure. Theoretically, this makes the structure to remain singly connected, in which case, the stress function constants of interior boundaries are no longer required. In practice, the treatment can be easily implemented via only assigning the property value of the candidate elements to a prescribed low value. Simple computer experiments reveal that such a "soft" core strategy does present a constant value of ϕ_i on an internal boundary.

For clarification, the torsion ESO procedure is organized as follows:

Step 1: Discretize the cross-sectional area using a dense FE mesh; define ESO driving parameter ER and RR_0;
Step 2: Carry out a FEA to solve the boundary value problem of Eqs. (1) and (2);
Step 3: Assign the shear moduli of candidate elements to a prescribed low value if their shear stress levels satisfy equation (6);
Step 4: If a *steady state* is reached, increase RR_{SS} by ER as Eq. (7) and set $SS = SS + 1$; repeat step 3; Otherwise, repeat steps 2 to 3 until an optimum is attained.

3.2. Procedure for the constant volume

In the previous situation, the optimization process was carried out by progressively removing least efficient material from the structure. Therefore, the total weight or the volume of the structure was gradually reduced during the evolutionary process. Sometimes, however, a designer may wish to improve the performance of a structure while keeping its weight (or volume or cross-section area) constant. This can be achieved by shifting material from the 'strongest' location to the 'weakest' location in a volume conserving manner. Through such a process, the less efficient (under-utilized) material becomes more efficient than before (over-utilized) until the best possible material distribution is attained.

To implement the procedure, an appropriate initial shape is modeled, where the solid and void regions are represented by a relatively high and a relatively low material property respectively. In terms of the shear stress levels as identified in Eq. (6), a small number of under-utilized elements are removed from the torsion section by switching their material property to the void one. Meanwhile, the same number of void elements with the highest stress levels are switched to the solid property. As a result, this process maintains the number of solid elements unchanged at each iteration.

It is worth pointing out that, in this process, although the void elements are theoretically expected to carry no torque, the numerical computation always results in a certain stress level due to the non-zero void material property. In most of the void elements, such virtual stress levels are close to zero except for those connected to solid ones where an appropriate extrapolation is automatically achieved to maintain a continuous change of torsion field in FE computation. The high virtual stresses in such attachment elements indicate the need to increase the solid material. In this sense, the virtual stress levels form a criterion to justify which void elements should be switched to solid ones.

For clarification, the torsion ESO procedure subject to the constant volume/cross-sectional area is given as follows:

Step 1: Discretize the design domain of cross-sectional area using a dense FE mesh; the initial solid and void regions are represented by high or low shear moduli respectively, and define ESO driving parameter ER and RR_0;

Step 2: Carry out a FEA to solve the boundary value problem of Eqs. (1) and (2);
Step 3: Switch the shear modulus of candidate solid elements to the void one if their shear stress levels satisfy Eq. (6), and then change a number of void elements with the highest virtual stress levels to solid ones while maintaining the cross-sectional area unchanged;
Step 4: If a *steady state* is reached, increase RR_{SS} by ER as Eq. (7) and set $SS = SS + 1$; repeat step 3; Otherwise, repeat steps 2 to 3 until an optimum is attained.

4. Illustrative examples

To demonstrate the torsion ESO procedures, five typical and practical design examples of torsional shafts are presented here. The evolutionary processes for all examples are driven by the initial rejection ratio of $RR_0 = 0\%$ and the evolution rate of $ER = 1\%$. In the pictures shown below, the black or dark areas represent the remaining solid elements and the small dots represent the nodes of the initial FE model. In all design processes, the twist angle per unit length is maintained at $\theta = 0.5°$, regardless of changes in the material volume or distribution.

4.1. Benchmarking example subject to area reduction

In the first example, the initial design domain is fully populated with solid elements in a square of 80×80 mm^2. A mesh of 40×40 four node quadrilateral elements is adopted to model the analysis domain as illustrated in Fig. 2(a).

4.1.1. Case 1: Exterior boundary design

As the first case, the element removal is limited to the outer boundary only. Therefore, the entire evolution process does not change the connectivity of the analyzed cross-section. Figs. 2(b)–(d) display the

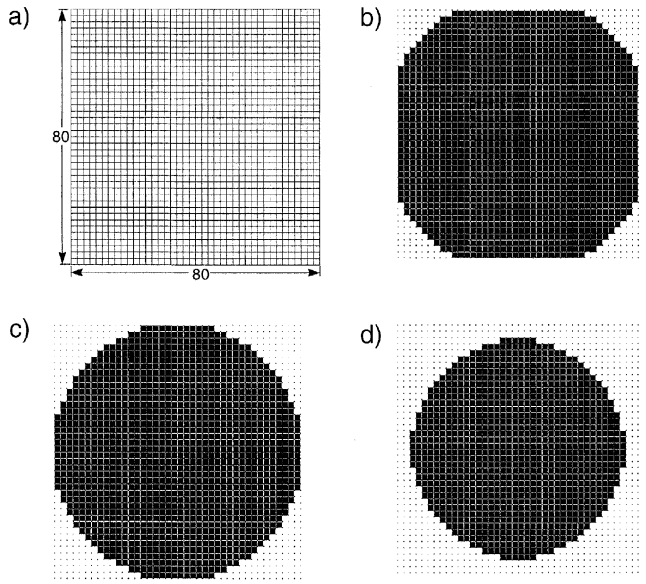

Fig. 2. Exterior boundary design via element removal: (a) initial design model, (b) $V/V_0 = 90\%$, iteration 18 or $SS = 12$, (c) $V/V_0 = 80\%$, iteration 36 or $SS = 18$ (form a circular profile) and (d) $V/V_0 = 60\%$, iteration 57 or $SS = 21$ (maintain circular profile).

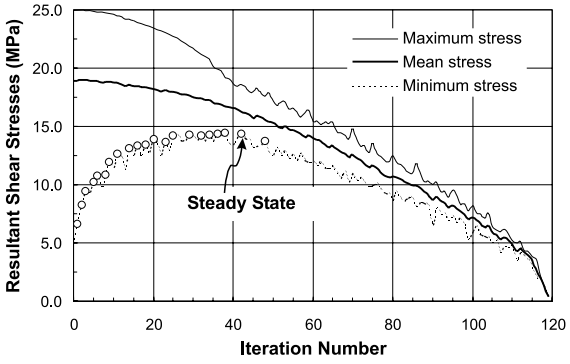

Fig. 3. Evolution histories of the resultant shear stresses.

process of material removal at the volume ratios of 90%, 80% and 60% respectively (the ratio of current solid volume/area to the initial solid volume/area).

To monitor the stress levels on the design boundary, the evolution histories of the maximum, mean and minimum shear stresses are plotted in Fig. 3. As the less stressed material is progressively removed from the section, it can be seen the difference between maximum and minimum stresses gets smaller and smaller until a circular outer profile is formed at iteration 36, in which the volume ratio and steady state number correspond to 80% and 18. After that, the deviation between the maximum and the minimum stress levels becomes relatively stable. As a result, a series of circular profiles with different sizes is generated as shown in Fig. 2(c) and (d). Theoretically, the deviation between the maximum and the minimum should be equal to zero for an *evenly stressed* shape. However, for a fixed grid approach like ESO, it is hardly possible to obtain such a perfect iso-stressed profile due to the approximation of the smooth boundary by a jagged profile and the imposition of the non-smooth boundary condition. Consequently, a constant deviation has indicated a stable state for the shaped profiles. Besides, from Fig. 3 one can also find that an ESO Steady State always appears at a stage with the minimum shear stress difference among all iteration steps between two Steady States. This implies that each ESO steady state can be an optimized solution.

On the other hand, although such optimal process is driven by the criterion of the shear strength, the result is also found to be in good agreement with the rigidity criterion by Polya (1948), in which a circular bar proves to have the highest torsional stiffness among all singly connected convex geometry. This means that a fully stressed design and a most rigid design share the same optimum profile. The following examples will provide more evidence on such an interesting feature.

4.1.2. Case 2: Interior boundary design

To observe the formation of multiply-connected sections, in this case, any possible internal boundary is allowed to be created but the outer boundary is preserved unchanged. This can be achieved by gradually switching the solid inner elements to void ones on the basis of stress levels. At the same time, the elements on the outer perimeter are unavailable for alteration. Fig. 4(a) and (b) display the process of internal material removal at volume ratios of 80% and 60%. It can be seen that when an inner profile is far from the outer boundary, a circular shape is obtained, but when the inner profile approaches to the exterior boundary, an approximate constant thickness profile emerges, which is consistent with the "shear flow" theory of thin walled tubes.

4.1.3. Case 3: Design for both exterior and interior boundaries

As the third example, both exterior and interior boundaries are allowed to change. Fig. 5(a)–(d) show the process of material removal at several specific volume ratios and Fig. 6 plots the evolution histories of

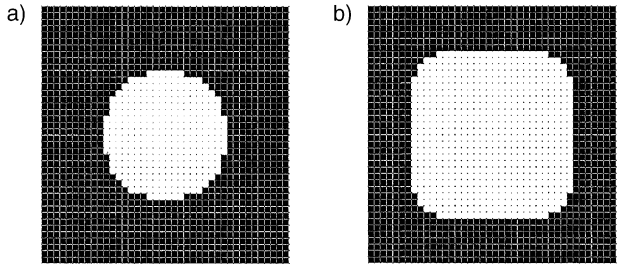

Fig. 4. Interior profile design via material removal: (a) $V/V_0 = 80\%$, iteration 37 or SS = 20 (form a circular hole) and (b) $V/V_0 = 60\%$, iteration 62 or SS = 25 (form an offset profile of outer boundary).

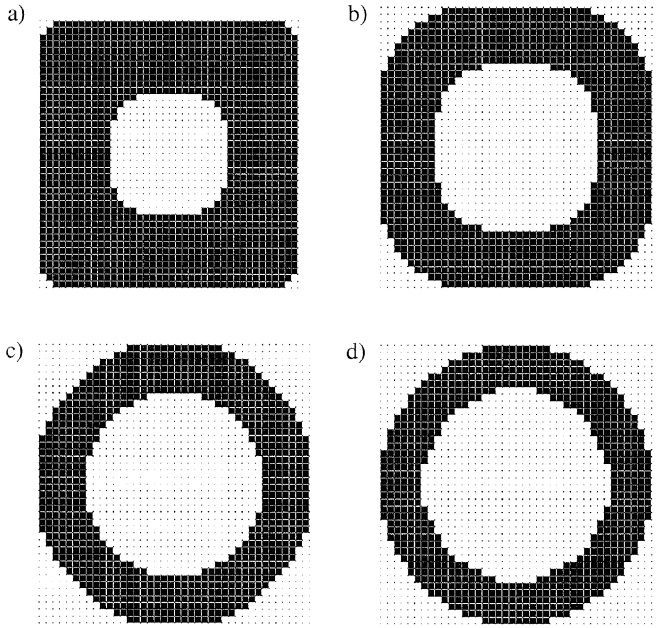

Fig. 5. Both inner and outer boundary design via element removal: (a) $V/V_0 = 80\%$ (steady state 17), (b) $V/V_0 = 60\%$ (steady state 23), (c) $V/V_0 = 50\%$ (steady state 28) and (d) $V/V_0 = 42\%$ (steady state 29).

the shear stresses. It can be observed that, as more and more inefficient material is removed from the structure, the deviation between the maximum and the minimum stresses becomes smaller and smaller. During the optimization process, the maximum stress progressively reduces while the minimum stress gradually increases. At a certain stage (around $V/V_0 = 42\%$), the minimum stress reaches its extreme and no longer increases. At this point, a circular ring is formed as shown in Fig. 5(d). Afterwards, both the maximum and the minimum stresses decrease in an approximately constant ratio except for the last few iterations, which represents a stable state where the stresses on the design boundaries are almost uniform. As a result, a series of rings with different sizes are produced. In the last few iterations, the drastic changes in stress deviation and rigidity just indicate a non-stable state, in which too many elements have been removed. As a result, with so few elements remaining, the zig-zag boundary causes significant shear stress jumps.

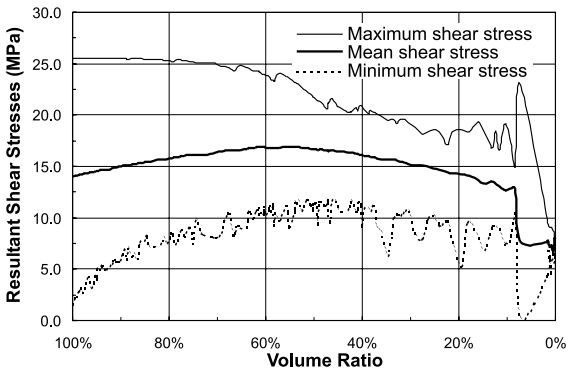

Fig. 6. Evolution histories of shear stresses.

From Polya and Weinsten's proof (Polya and Weinsten, 1950), in the cases of multiply connected cross-sections, a ring bounded by two concentric circles has the highest torsional stiffness. It is interesting to notice that the result produced from the fully stressed criterion is in excellent agreement with such a rigidity criterion. To observe the rigidity change, the relation between rigidity and volume is plotted in Fig. 7. In the early stages of evolutionary material removal, the volume reduction exceeds the rigidity reduction. Therefore the torsional stiffness efficiency (stiffness/area) of the section grows with the material removal. This results in equal thick walled geometry being formed progressively. However, after a certain volume ratio, the rigidity reduction gradually overtakes the volume reduction. It is interesting to note that the extreme of the rigidity–volume curve appears at the volume ratio of 60%, which corresponds to the topology with an equal thick wall as shown in Fig. 5(b) rather than the annulus as shown in Fig. 5(c) and (d). This is not in contradiction to Polya and Weinsten's proof rather, for a given area, when there is no limitation to design space, a perfect thin ring always gives the optimum rigidity for multiply-connected topologies. The design case in Section 4.2.3 of the next example will demonstrate this point better. In the present example, however, the evolution process is considerably affected by the design domain. It will be shown that only when the rejection ratio reaches a certain level, such influence can be excluded. For this reason, the rigidity–volume curve only provides an indication of rigidity efficiency subject to a specific design space.

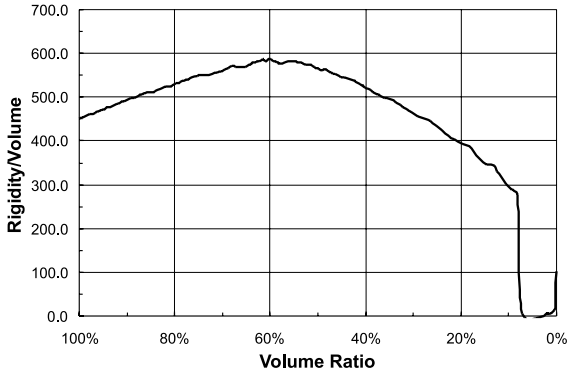

Fig. 7. Evolution histories of rigidity vs volume.

4.2. Benchmarking example subject to constant volume

In this example, some initial guesses of the design shapes are modeled in terms of solid elements and void elements respectively. Similarly to the previous example, the design domain is constrained with a square of 80×80 mm^2. A mesh of 40×40 four node quadrilateral elements is used to discretize the analysis domain.

4.2.1. Case 1: Exterior boundary design

In this case, the exterior boundary is considered as the design target. A greek cross shape is given as the initial design as illustrated in Fig. 8(a). In the evolution process, the solid elements on the outer boundary are progressively moved from under-utilized (lowly stressed) locations to over-utilized (highly stressed) locations. Fig. 8(b)–(d) show the modification process of the exterior boundary. It can be seen that the outer boundary gradually forms a circle as shown in Fig. 8(d).

The deviation between the maximum and minimum boundary stress is plotted in Fig. 9. It can be seen that, as material is shifted, the deviation gets smaller and smaller until a circular profile forms. Subsequently, the shear stress deviation varies in an oscillatory manner as shown in Fig. 9, which indicates the circular profile is a stable design state to which no further improvement can be made. As a result, for singly connected design domains, the circular profile yields a uniform stress distribution on the outer boundary. More examples can be given to provide further evidence that, for different singly connected geometries with a given area, only the circular profile presents the uniform stress distribution in the design boundary. Note that this inference is exactly the same as the result from rigidity criterion by Polya (1948). In this sense, the circular bar has both strength and rigidity advantages over all other shapes.

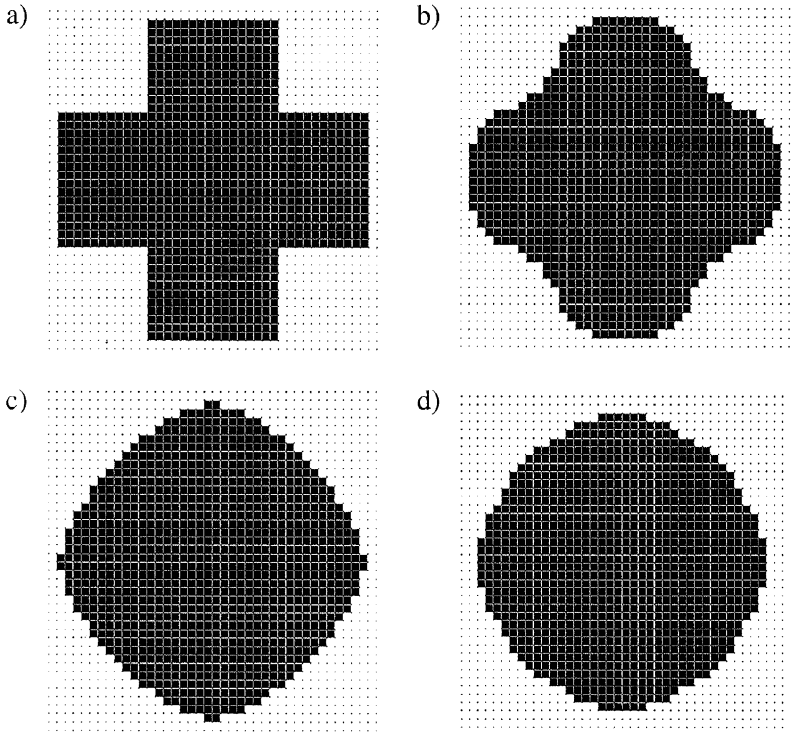

Fig. 8. Optimal exterior boundary design subject to constant volume: (a) initial design, (b) iteration 8 or steady state 5, (c) iteration 18 or steady state 10 and (d) final design (a circle).

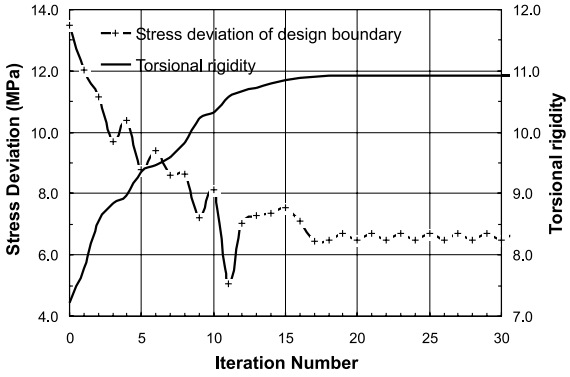

Fig. 9. Evolution histories of shear stress deviation and torsional rigidity.

4.2.2. Case 2: Interior boundary design

As with the analysis of Section 4.1.2, only inner holes or boundaries are allowed to be created in this case. To observe the evolution process with an initial non-symmetrical geometry, a square hole is eccentrically located in the initial design domain as shown in Fig. 10(a). The process of material shifting is displayed in Fig. 10(b)–(d). It can be seen that, during the optimization procedure, the centroid of the internal hole is progressively moved from its initial position towards a symmetric location in relation to the exterior boundary.

From the evolution histories of shear stress deviation and torsion rigidity changes as given in Fig. 11, it can be identified that a circle located at the symmetric center of section (as shown in Fig. 10(d)) corresponds

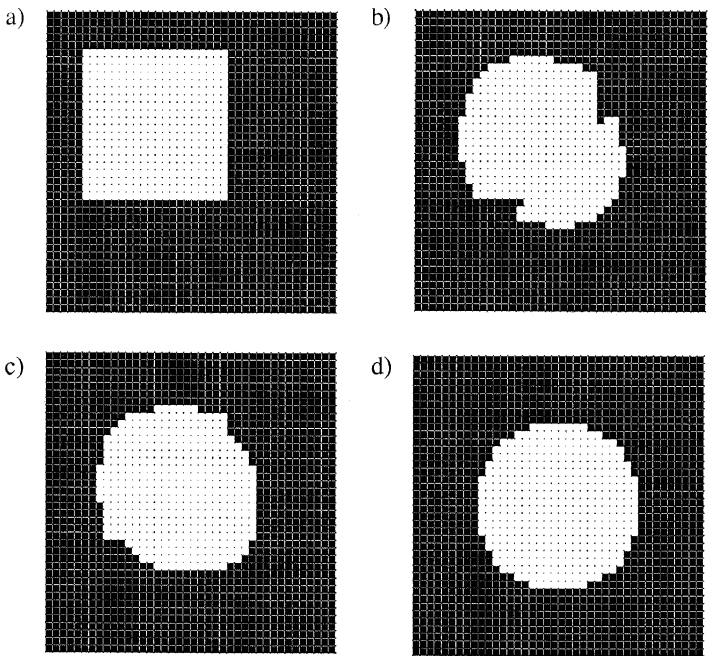

Fig. 10. Optimal interior boundary design subject to the constant volume: (a) initial design, (b) iteration 10 or steady state 5, (c) iteration 23 or steady state 10 and (d) final design (iteration 55 or steady state 25).

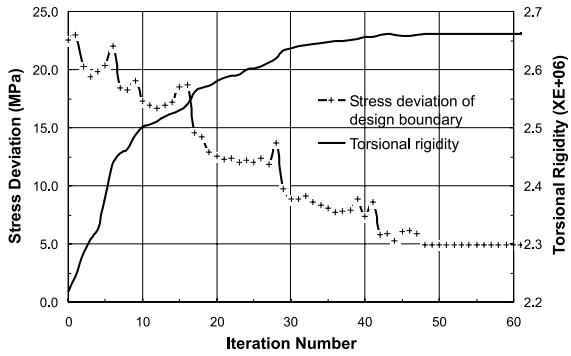

Fig. 11. Evolution histories of shear stress deviation and torsional rigidity.

to the stable status of both the shear strength and the torsional rigidity. This shows that, for doubly-connected design domains, when the solid and void areas have the same centroid, the section has both the highest torsional rigidity and the most uniform shear stress distribution.

At this point, it could be asked if the strength and rigidity can be improved further by increasing the connectivity value of the cross-section. To answer this question, one more case with four initial internal holes is demonstrated as shown in Fig. 12(a). With the evolution process, more and more solid elements are shifted to locations most remote from the symmetric center of the section, while more and more void elements appear in the central area. This is due to the fact that material gradually migrates from the 'strongest' location to the 'weakest' location. Thus, such a quintuply-connected initial domain (four inner holes) automatically degenerates to a doubly-connected field (one centrally located circular hole). It shows

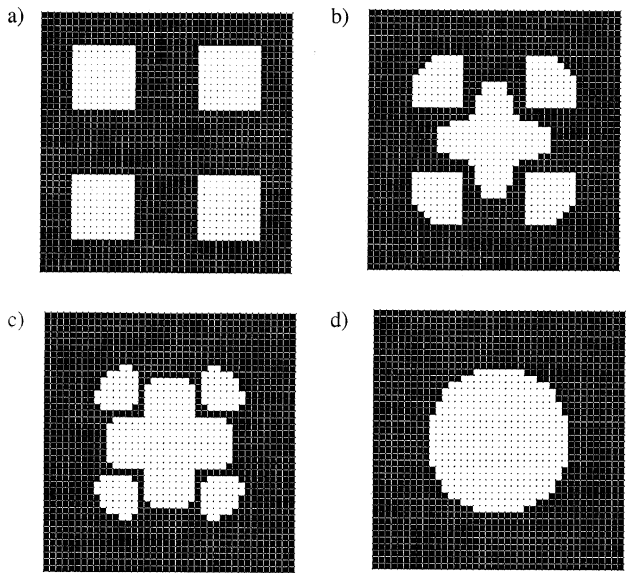

Fig. 12. Optimal interior boundary design subject to constant volume: (a) initial design, (b) iteration 34 or steady state 5, (c) iteration 49 or steady state 10 and (d) final design (iteration 68 or steady state 20).

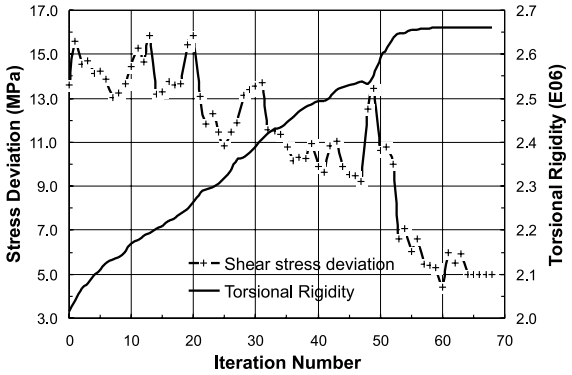

Fig. 13. Evolution histories of shear stress deviation and torsional rigidity.

that a single circular hole can best satisfy the iso-strength criterion. Also, from the stiffness viewpoint, it can be identified that the section with a circular hole has the better rigidity than multiply-connected domain as shown in Fig. 13. Such a conclusion is in excellent agreement with that of Gracia and Doblare's investigation (1988).

4.2.3. Case 3: Design for both exterior and interior boundaries

In this case, both exterior and interior boundaries are allowed to reform. It is expected to investigate that, for a given area, what shape has a most uniform stress distribution. As illustrated in Fig. 14(a), a 56×56 mm^2 singly-connected solid square bar (meshed by 28×28 elements) is considered as the initial

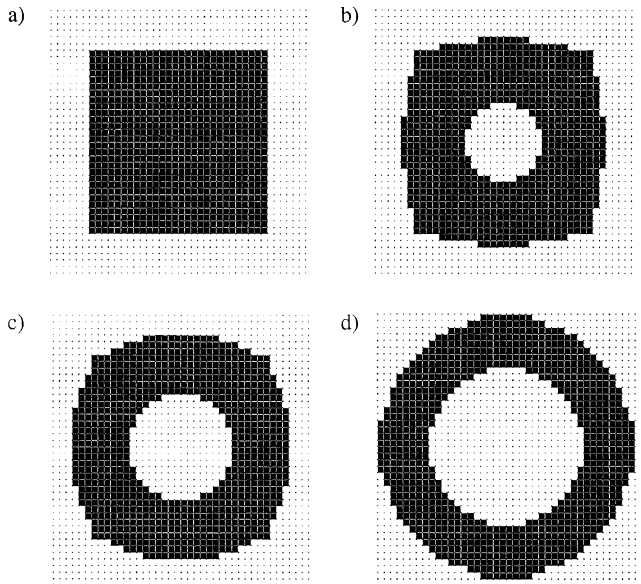

Fig. 14. Optimal both exterior and interior boundary design subject to constant volume: (a) initial design, (b) iteration 15 or steady state 10, (c) iteration 25 or steady state 13 and (d) final design (iteration 48 or steady state 20).

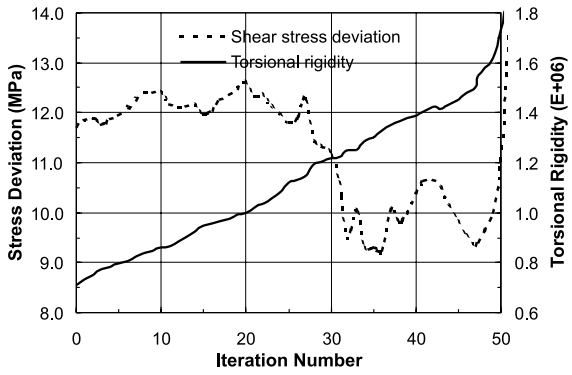

Fig. 15. Evolution histories of shear stress deviation and torsional rigidity.

design. Fig. 14(b)–(d) display the reorganization process of the solid material. Since the shorter the distance of an element to the section centroid, the lower its shear stress level, this leads to more and more solid elements migrating from interior region to the available exterior. As a result, a circular hole is gradually created at the central area while the straight edges of the exterior profile are progressively encircled. After a certain number of evolutionary cycles, an annulus with two concentric circles is formed, which represents the 'lowest' stable state as shown in Fig. 14(b). Beyond this point, the evolution process produces no more topological changes, rather a series of different sized rings is formed as displayed in Fig. 14(c) and (d). From these figures, one can see the wall of the ring become thinner and thinner as the evolution process proceeds. Accordingly, the deviation of shear stress levels becomes smaller and smaller as shown in Fig. 15. If the design domain is large enough, the process would ultimately result in a 'thin-walled' ring, in which the shear stress levels on the interior and the exterior boundaries become almost identical. In fact, this represents the ideal iso-strength topology.

Furthermore, from the stiffness viewpoint, it can be seen that a larger ring indeed possesses a higher torsional rigidity for a given area as illustrated in Fig. 15. In this example, the design space is considerably larger than the given solid area, which allows such a design to be achieved in a bigger space. This also answers the question raised in Section 4.1.3 that, when design space is large enough, the shape of the ring is always formed to that with the maximum rigidity among all possible geometries. In this sense, the optimization of strength and rigidity can be achieved simultaneously. In other words, a ring bounded by two concentric circles has both the most uniform stress distribution and the highest torsional stiffness for any possible multiply connected cross-section.

In fact, the design shown in Fig. 14(d) represents the last ESO steady state that can be achieved in such a specific design domain. After such a steady state (SS = 20), further iteration will result in a non-circular thin ring. As shown in the last several iterations in Fig. 15, although the rigidity increases further, the deviation of shear stresses becomes worse. This indicates that the design domain limits to achieve a new ESO steady state.

4.3. Effect of exterior boundaries on multiply-connected design

The third example presents some outer boundary variations and shows the effect of these on the optimized inner boundary shapes. The example gives two different cases of outer boundaries as Fig. 16(a) and (b). In the Greek cross shaft case, a concavely edged square with a 45° angle to the global coordinate system has resulted. While in the octagonal shaft case, a concentric octagon with the same major axes as the

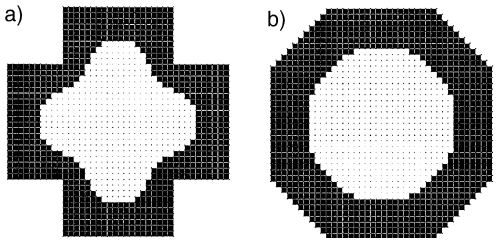

Fig. 16. Effects of exterior boundaries on the optimal inner shapes: (a) cross shaft and (b) octagonal shaft.

exterior boundary is produced. Obviously, the outer boundaries have a significant effect on the inner ones, in particular, when the inner boundary is close to the outer one. Indeed, the migration of the interior boundary follows a path to make the gradient of the stress function more uniform. Obviously, a design with almost equal thickness wall can best reflect the stress based optimality criterion.

4.4. Example of multiple material shafts

This example presents the design cases of the shafts composed of two isotropic elastic materials with different shear moduli. In this example, two configurations of material combinations are considered as shown in Fig. 17(a) and (b) respectively. It can be clearly seen that, to achieve the equal strength design, the stronger material (with higher shear modulus) needs less volume than the weaker one. From the torsional rigidity point of view, likewise, the stiffer material (with higher shear modulus) needs less volume than the flexible material (with lower shear modulus) to produce uniform shear deformation.

4.5. Example of keyway designs

In practice, a designer frequently needs to consider a hollow shaft with a groove(s) required for a keyway(s). The task could involve the determination of an optimal interior boundary shape from a strength and rigidity point of view. Shown in Fig. 18(a)–(d) are the design cases of circular hollow shafts with the exterior grooves, in which 1, 2, 4 and 6 exterior keyways are taken into account respectively. Through the case of the single groove as shown in Fig. 18(a), it can be seen that the strength-driven topology is similar to the rigidity based one by Hou and Chen (1985). This provides further evidence to indicate that iso-strength design can share the same optimum shape with the stiffest one (Li et al., 1999c). The remaining pictures shown in Fig. 18(b)–(d) present more solutions for multiple groove cases of such typical design problems leading to many keyways which could be seen to be similar to gear teeth.

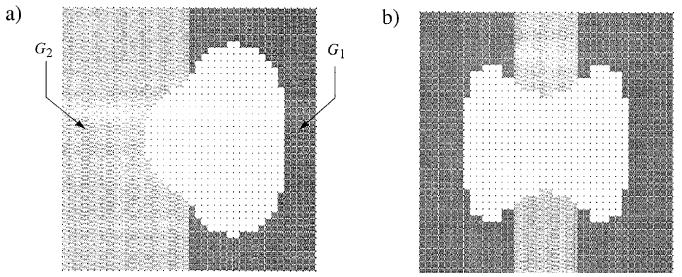

Fig. 17. Design of shafts made by two materials ($G_1/G_2 = 3$): (a) two layers and (b) three layers.

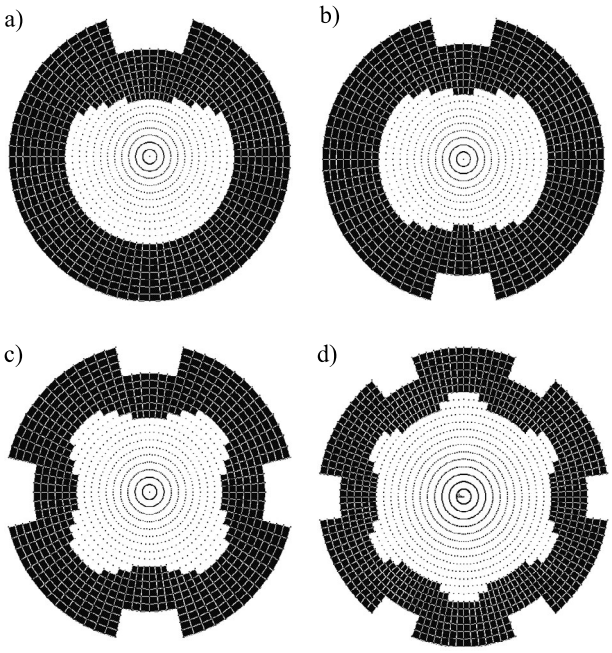

Fig. 18. Circular hollow shafts with the exterior keyways: (a) single keyway, (b) two keyways, (c) four keyways and (d) six keyways.

5. Concluding remarks

This paper presents an ESO method for solving the shape design problem of shafts experiencing pure torsional load. From the iso-strength point of view, the optimality criterion is determined in terms of the resultant shear stress level of FE of the cross section area due to torsion. To meet different design requirements, two approaches are developed, firstly by gradually removing less efficient material from a fully populated design domain and secondly by progressively migrating material from the strongest location (least necessary) onto the weakest location (most necessary). These two procedures have been well demonstrated through a series of typical examples.

One of the distinct advantages of the present evolutionary method over classical ones is that it does not involve any complicated mathematical operations and programming, nor does it require profound knowledge of the FEA. Typically, a designer is capable of using the FE packages proficiently, but does not have to access the source code of the FE program. To implement the presented ESO procedure, the user does not need to know more than the basic output of elemental resultant shear stress and the standard input of material properties of a FE model. In fact, when considering the analogy in the governing equations between heat transfer and torsion problems, the Poisson equation can be solved via a heat solver included in any FE programs, in which the values of temperature and heat fluxes can be translated into stress function and shear stress level respectively (Li et al., 1999a and Steven et al., 2000). This makes the presented method to be of wide suitability and generality.

By comparing the optimum shapes resulting from the iso-strength criterion with those from the rigidity criterion, a physical resemblance can be identified. This means that a fully stressed design and a most rigid design can share the same geometry. To a certain extent, the stiffest design may be accomplished via a fully stressed design, or vice versa. This provides a useful alternative for designers to deal with these two different design criteria.

References

Adali, S., 1981. Cross-sectional shape of an anisotropic, hollow bar with maximum torsional stiffness. Engng. Optim. 5, 169–177.

Banichuk, N.V., 1976. Optimization of elastic bars in torsion. Int. J. Solids Struct. 12, 275–286.

Banichuk, N.V., Karihaloo, B.L., 1976. Minimum-weight design of multipurpose cylindrical bars. Int. J. Solids Struct. 12, 267–273.

Bendsøe, M.P., 1995. Optimization of Structural Topology, Shape, and Material. Springer, Berlin, New York.

Burns, T., Cherkaev, A., 1997. Optimal distribution of multimaterial composites for torsional beams. Struct. Optim. 13, 4–11.

Dems, K., 1980. Multiparameter shape optimization of elastic bars in torsion. Int. J. Numer. Meth. Engng. 15, 1517–1539.

Gracia, L., Doblare, M., 1988. Shape optimization of elastic orthotropic shafts under torsion by using boundary elements. Comp. Struct. 30, 1281–1291.

Hinton, E., Owen, D.R.J., 1981. An Introduction to Finite Element Computations. Pineridge Press, England.

Hinton, E., Sienz, J., 1995. Fully stressed topological design of structure using an evolutionary procedure. Engng. Comp. 12, 229–244.

Hou, J.W., Chen, J.L., 1985. Shape optimization of elastic hollow bars. ASME Trans.: J. Mech. Transm. Autom. Des. 107, 100–105.

Huston, R.L., Passerello, C.E., 1984. Finite Element Methods, An Introduction, Marcel Dekker, New York.

Karihaloo, B.L., Hemp, W.S., 1983. Minimum weight thin walled cylinders of given torsional and flexural rigidity. ASME Trans.: J. Appl. Mech. 50, 892–894.

Karihaloo, B.L., Hemp, W.S., 1987. Optimum sections for given torsional and rigidity. Proceedings of Royal Society, London, A 409, pp. 67–77.

Kim, Y.Y., Kim, T.S., 2000. Topology optimization of beam cross sections. Int. J. Solids Struct. 37, 477–493.

Li, Q., Steven, G.P., Querin, O.M., Xie, Y.M., 1999a. Evolutionary optimization for cross-sectional shape of torsional shafts, In: Proceeding of Third World Congress on Structural and Multidisciplinary Optimization WCSMO-3, CD Volume, New York.

Li, Q., Steven, G.P., Querin, O.M., Xie, Y.M., 1999b. Shape and topology design for heat conduction by evolutionary structural optimization. Int. J. Heat Mass Transf 42, 3357–3367.

Li, Q., Steven, G.P., Xie, Y.M., 1999c. On equivalence between stress criterion and stiffness criterion in evolutionary structural optimization. Struct. Optim. 18, 67–73.

Lurie, K.A., Cherkaev, A.V., Fedorov, A.V., 1982. Regularization of optimal design problems for bars and plates, part 1. J. Optim. Theory Appl. 37, 499–522.

Mioduchowski, A., Faulkner, M.G., Kim, B., 1989. Optimal solutions for non-homogeneous multiply-connected torsional sections. ASME J. Mech. Trans. Automat. Des. 111, 87–93.

Mota Soares, C.A., Rodrigues, H.C., Oliverira, L.M., Mota Haug, E.J., 1984. Optimization of the geometry of shafts using boundary elements. ASME J. Mech. Trans. Automat. and Des. 106, 199–203.

Parbery, R.D., Karihaloo, B.L., 1977. Minimum-weight design of hollow cylinders for given lower bounds on torsional and flexural rigidities. Int. J. Solids Struct., 13,1271–1280.

Parbery, R.D., Karihaloo, B.L., 1980. Minimum-weight design of thin walled cylinder subject to flexural and torsional stiffness constraints. ASME Trans.: J. Appl. Mech. 47, 106–110.

Polya, G., 1948. Torsional rigidity, principal frequency, electrostatic capacity and symmetrization. Quart. Appl. Math. 6, 267–277.

Polya, G., Weinstein, A., 1950. On the torsional rigidity of multiple connected cross-sections. Annals Math 52, 154–163.

Rao, S.S., 1989. The Finite Element Method in Engineering. Pergamon Press, New York.

Schramm, U., Pilkey, W.D., 1993. Structural shape optimization for the torsion problem using direct integration and B-splines. Comp. Meth. Appl. Mech. Engng. 107, 251–268.

Schramm, U., Pilkey, W.D., 1994. Higher order boundary elements for shape optimization using rational B-splines. Engng. Anal. Boundary Elements 14, 255–266.

Steven, G.P., Li, Q., Xie, Y.M., 2000. Evolutionary topology and shape design for mathematical physical problems. Computat. Mech. 26, 129–139.

Xie, Y.M., Steven, G.P., 1993. A simple evolutionary procedure for structural optimization. Comp. Struct. 49, 885–896.

Xie, Y.M., Steven, G.P., 1997. Evolutionary Structural Optimization, Springer, Berlin.